ACS OMEGA

http://pubs.acs.org/journal/acsodf

Article

Lysosome-Targeting Fluorescence Sensor for Sequential Detection and Imaging of Cu^{2+} and Homocysteine in Living Cells

Lihua Liu, Hongfei Duan, Haohui Wang, Jieru Miao, Zhihui Wu, Chenxi Li, and Yan Lu*

Cite This: *ACS Omega* 2022, 7, 34249−34257

Read Online

ACCESS | Metrics & More | Article Recommendations | Supporting Information

ABSTRACT: A conjugated polymer-based fluorescence sensor, namely, PTNPy, was constructed on the basis of a polythiophene scaffold coupled with dimethylpyridylamine (DPA) groups in side chains for the consecutive detection and quantification of Cu^{2+} and Hcy in a perfect aqueous medium. A dramatic fluorescence quenching of PTNPy by the addition of Cu^{2+} was observed in Tris−HCl buffer solution (2 mM, pH 7.4), demonstrating a quick (<1 min) and highly selective response to Cu^{2+} with a low limit of detection of 6.79 nM. Subsequently, the Cu^{2+}-quenched fluorescence of PTNPy can be completely recovered by homocysteine (Hcy), showing excellent selectivity to Hcy over other competitive species such as cysteine and glutathione. Thanks to the low cytotoxicity and lysosomal targeting ability of PTNPy, it was further applied as an optical sensor for the sequential imaging of Cu^{2+} and Hcy in HeLa cells. More importantly, Hcy concentration was linearly related to the fluorescence intensity of PTNPy in living cells, demonstrating huge potential for real-time monitoring the fluctuation of Hcy levels in living cells.

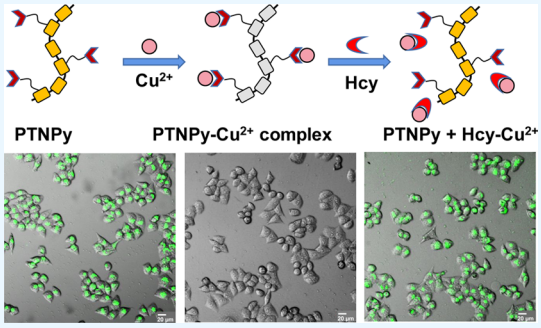

1. INTRODUCTION

Biothiols mainly including homocysteine (Hcy), cysteine (Cys), and glutathione (GSH), as well as various metal ions such as Cu^{2+}, Fe^{2+}, Ca^{2+}, and so forth, are well known to be involved in many biological processes and play key roles in human physiology.[1−5] Their levels in human plasma have already been directly or indirectly linked to many diseases.[6−11] For instance, the concentration of Hcy in body fluids is normally of 12−15 μM, and an elevated level is related to many human afflictions such as cardiovascular disease, Alzheimer's diseases, stroke, cancer, and so on.[12,13] More importantly, it was observed that the levels of copper and Hcy simultaneously elevate in patients with cardiovascular disease.[14,15] Kang et al. demonstrated that Hcy interferes with Cu homeostasis and hampers the availability of copper to chaperones such as cytochrome-c oxidase and COX17, resulting in mitochondrial dysfunction and endothelial cell injury.[16] Jakubowski and co-workers also confirmed that copper promotes efficient demethylation of methionine (Met) to increase the Hcy levels.[17] In addition, O^{2-} produced by complexation of Hcy with Cu^{2+} can clear NO and inhibit NO-related cerebrovascular diseases.[18] Therefore, the specific and simultaneous detection of Cu^{2+} and Hcy especially at the cellular level is of importance to understand their physiological functions and clinically diagnose the related diseases.

Fluorescence sensors are regarded as the most charming method to real-time monitor and track biological species through combining with the laser confocal imaging technology due to its simplicity, sensitivity, and high temporal and spatial resolution.[19,20] In recent decades, a mass of fluorescence sensors has been developed to identify Hcy from other amino acids, especially structurally similar mercaptoamino acids such as Cys and GSH[21−27] by taking advantage of distinctive redox property of Hcy[21−23] or nucleophilic reactions based on −SH and/or $-NH_2$ of Hcy.[24−27] To date, however, only a few sensors can sequentially sense Cu^{2+} and Hcy[18,28−38] that usually operated in a mixed medium of organic solvent and water[18,28,29,31,32,34,35] and suffer from the interference from other analytes (Table S1).[28−32,34,36,37] Besides, there are rare sensors available for continuous imaging of Cu^{2+} and Hcy in living cells.[18] Thus, it is still urgently needed to develop bifunctional fluorescence sensors for the simultaneous detection of Cu^{2+} and Hcy with high sensitivity and selectivity in a prefect aqueous solution and living cells.

Thanks to high brightness, excellent light stability, and easily adjustable spectral characteristics, π-conjugated polymers have been widely used to construct sensing and imaging platforms for various bio-related analytes.[39,40] Zhang's group developed a polythiophene derivative (PTMA) with a tridentate N-/O-containing ligand for the recognition of heavy metal ions and biothiols in aqueous solutions.[37] The addition of Co^{2+}, Cd^{2+}, and Cu^{2+} can induce a dramatic fluorescence decrease of

Received: June 14, 2022
Accepted: September 6, 2022
Published: September 14, 2022

Scheme 1. (a) Synthetic Route of the Sensor PTNPy and (b) Schematic Diagram of the Sequential Fluorescence Response of PTNPy toward Cu^{2+} and Hcy

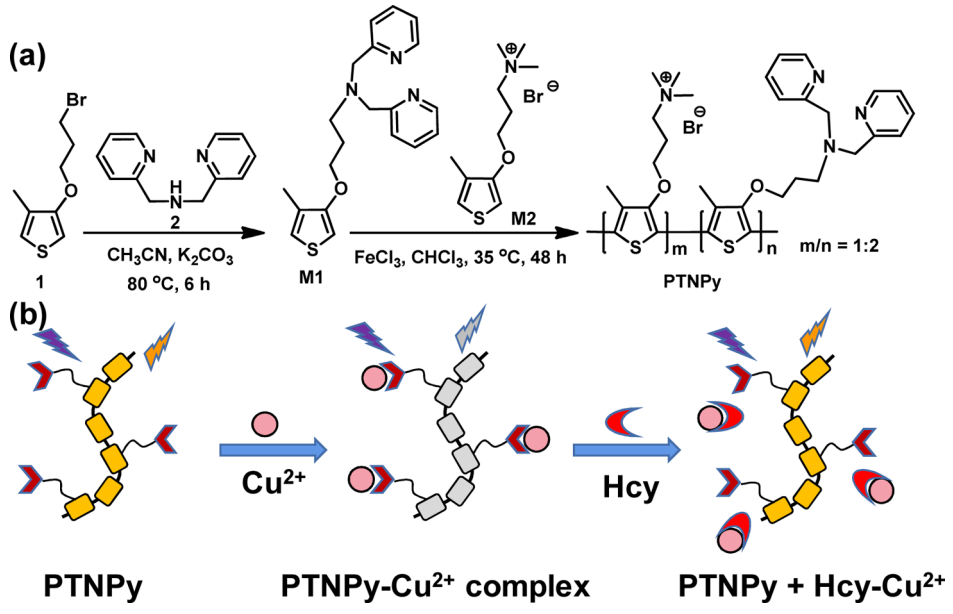

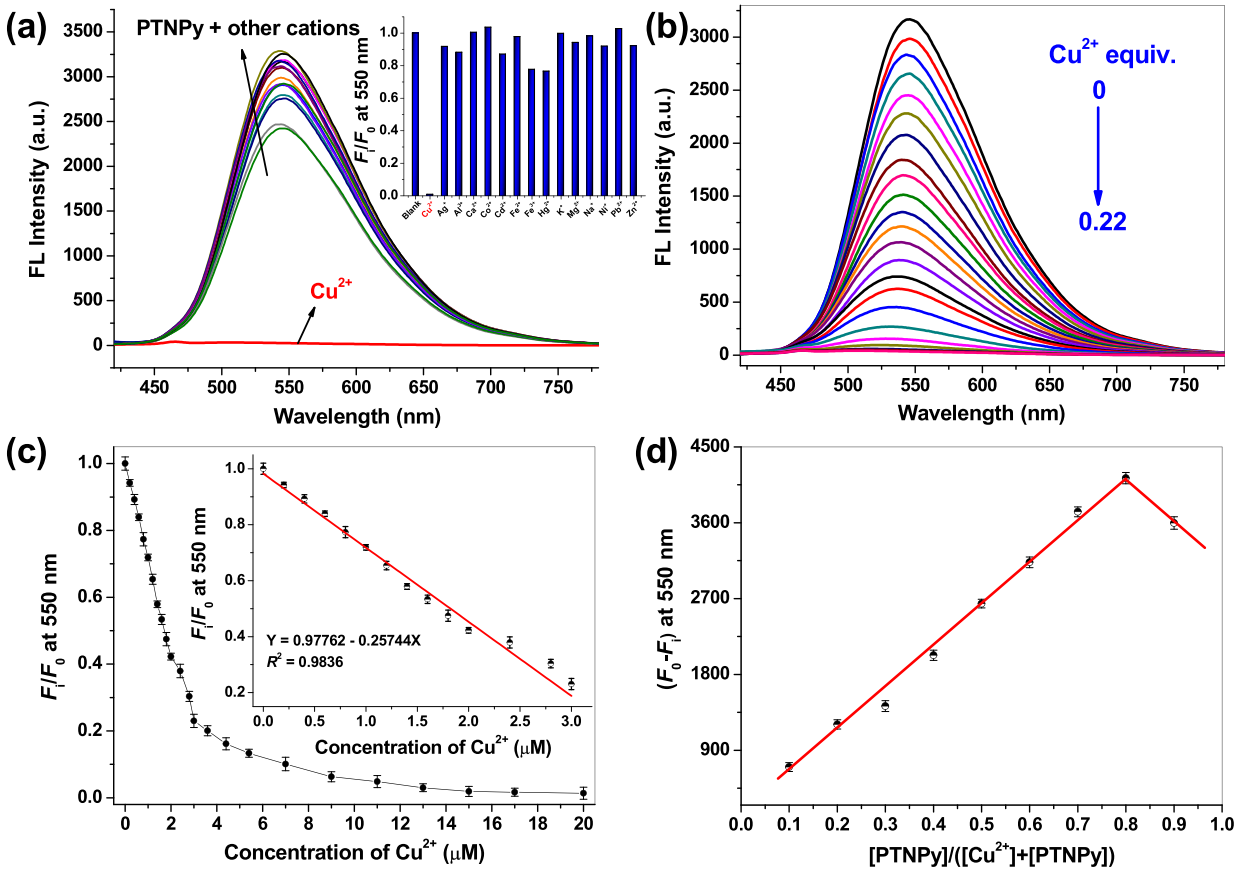

Figure 1. (a) Fluorescence spectra of PTNPy (100 μM) in Tris−HCl buffer solution (2 mM, pH 7.4) in the absence and presence of various tested metal ions (100 μM). Inset: ratio of fluorescence intensity (F_i/F_0) at 550 nm in the presence of various tested metal ions. (b) Fluorescence spectra of PTNPy (100 μM) in Tris−HCl buffer solution (2 mM, pH 7.4) with the amounts of Cu^{2+} (0−0.22 equiv). (c) Fluorescence intensity ratio (F_i/F_0) at 550 nm of PTNPy at 550 nm as a function of addition of Cu^{2+} amounts; the linearity of peak intensity with respect to Cu^{2+} concentrations (inset). The data were extracted from the titration curves (b). (d) Job's plot. F_0 and F_i denote the emission intensity at 550 nm prior to and after the addition of Cu^{2+} ions, respectively. λ_{ex} = 400 nm. Error bars represent the standard deviations of three trials.

PTMA, and subsequently, the Cu^{2+}-quenched fluorescence can be restored by Hcy and GSH with fluorescence enhancement of 11.5 and 7.7 folds in the THF/Tris−HCl mixed solution.[37] More recently, Tang's group reported a fluorene- and

https://doi.org/10.1021/acsomega.2c03691
ACS Omega 2022, 7, 34249−34257

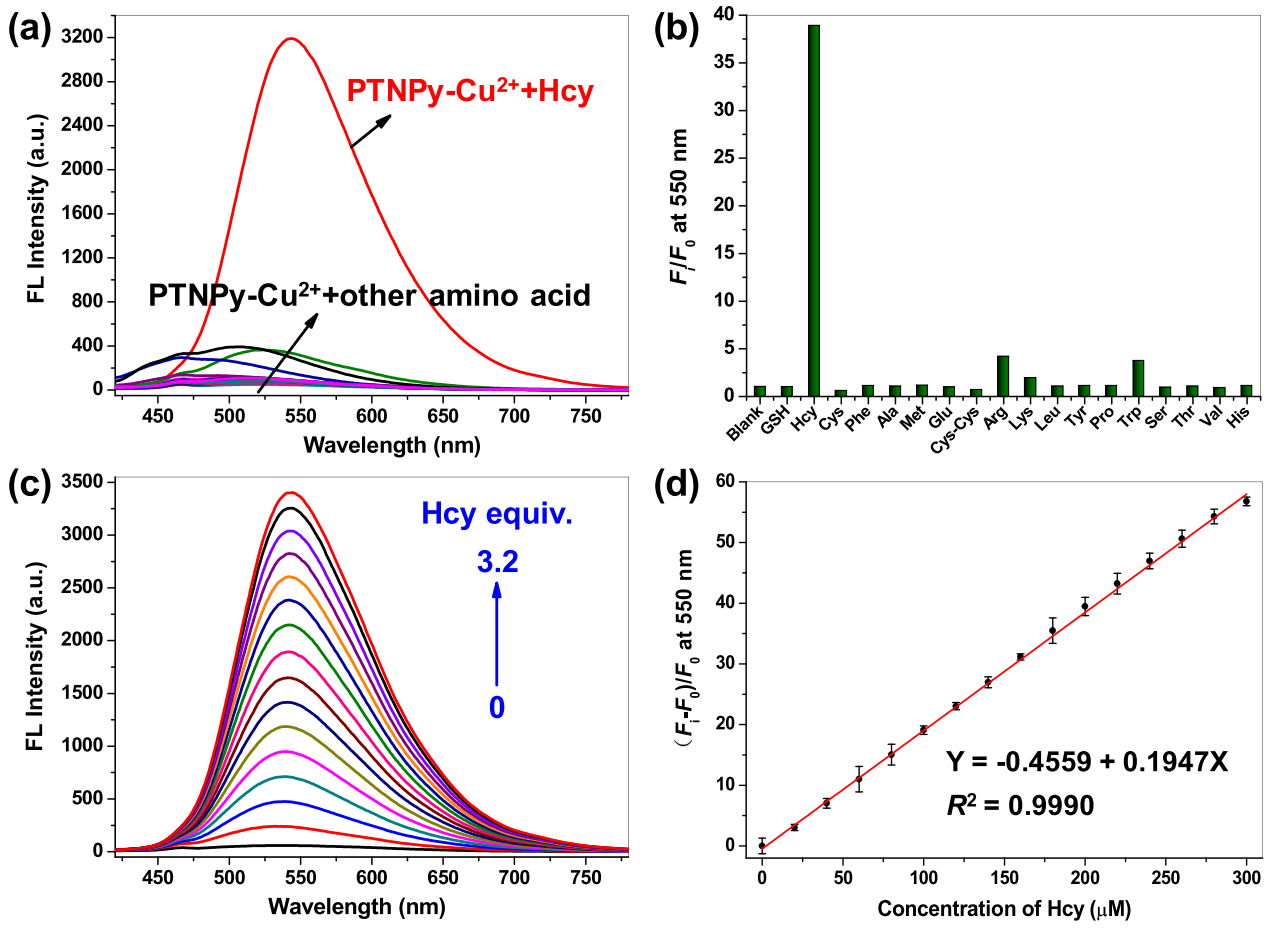

Figure 2. (a) Fluorescence spectra of PTNPy−Cu^{2+} complexes (100 μM) in Tris−HCl buffer (2 mM, pH 7.4) in the presence of 4 equiv of different amino acids and peptides. (b) Relative fluorescence intensity (F_i/F_0) at 550 nm of PTNPy−Cu^{2+} (100 μM) in Tris−HCl buffer (2 mM, pH 7.4) toward various tested amino acids, data were extracted from (a). (c) Fluorescence spectra of PTNPy−Cu^{2+} (100 μM) with the addition of various concentrations of Hcy (0−3.2 equiv) in Tris−HCl buffer (2 mM, pH 7.4). (d) Plot of $(F_i - F_0)/F_0$ at 550 nm vs concentrations of Hcy. F_0 is the initial emission intensity of PTNPy−Cu^{2+} complexes (100 μM), and F_i is the recorded emission intensities of PTNPy−Cu^{2+} complexes in the presence of Hcy with different concentrations. λ_{ex} = 400 nm. Error bars represent the standard deviations of three trials.

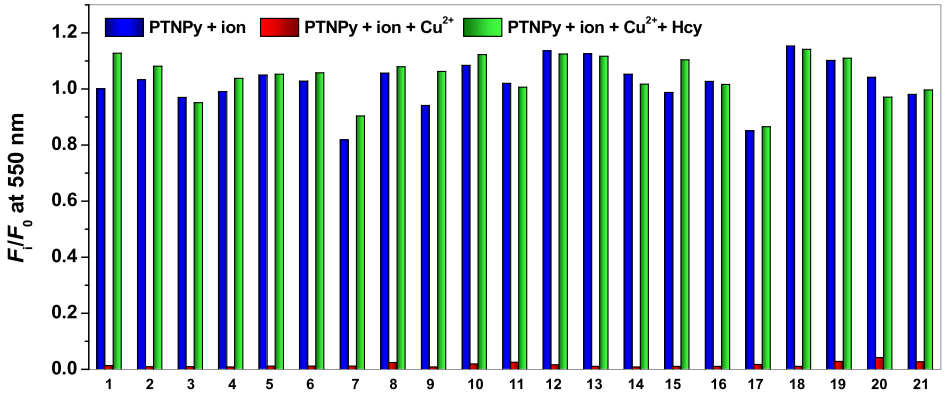

Figure 3. Competitive binding experiments of PTNPy (100 μM) in Tris−HCl buffer solution (2 mM, pH 7.4) with various bio-related species (100 μM) in the absence and presence of Cu^{2+} (20 μM) and Hcy (400 μM). 1: none, 2: Na^+, 3: Zn^{2+}, 4: Mg^{2+}, 5: K^+, 6: Fe^{2+}, 7: Fe^{3+}, 8: Ca^{2+}, 9: Cl^-, 10: CO_3^{2-}, 11: HCO_3^-, 12: $H_2PO_4^-$, 13: HPO_4^{2-}, 14: I^-, 15: NO_3^-, 16: OAc^-, 17: $P_2O_7^{4-}$, 18: PO_4^{3-}, 19: S^{2-}, 20: $S_2O_3^{2-}$, and 21: SO_4^{2-}.

benzothiadiazole-containing conjugated polymer-based fluorescence nanosensor, allowing imaging of Hcy levels in the kidney and liver of diabetic mice.[38]

Inspired by these outstanding works and the fact that there is a strong interaction between Cu^{2+} and Hcy,[41−44] herein, we reported a new conjugated polymer (PTNPy, Scheme 1a) as a multifunctional sensor for the goal of a quick, sequential detection of Cu^{2+} and Hcy in a perfect aqueous medium and living cells. PTNPy possess a polythiophene backbone as a fluorophore, dimethylpyridylamine (DPA) as the chelating groups of Cu^{2+} ions, and quaternary ammonium salt groups in its side chains to increase its water solubility. As shown in

https://doi.org/10.1021/acsomega.2c03691
ACS Omega 2022, 7, 34249−34257

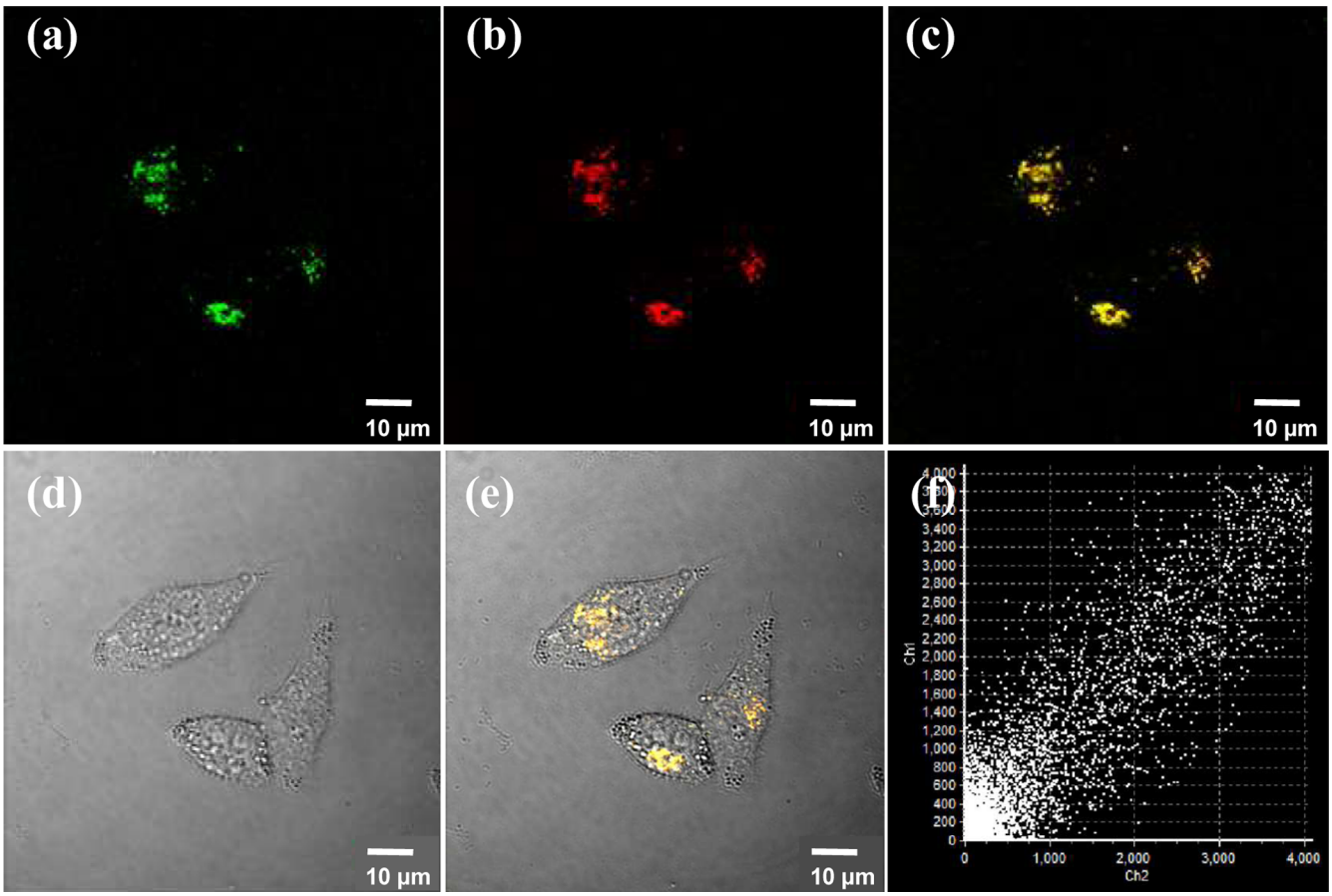

Figure 4. Colocalization of HeLa cells stained with PTNPy (20 μM) and LysoTracker Red. (a) PTNPy (20 μM) (λ_{ex} = 405 nm and λ_{em} = 496−554 nm). (b) LysoTracker Red (75 nM) (λ_{ex} = 559 nm and λ_{em} = 577−649 nm). (c) Merged image of (a,b). (d) Bright-field image. (e) Merged image of (c,d). (f) Pearson's overlap coefficient distribution. Scale bars: 10 μm.

Scheme 1b, the chelation of Cu^{2+} with the DPA groups of PTNPy led to the formation of stable PTNPy−Cu^{2+} complexes and thus effectively quenched the fluorescence of PTNPy due to the intrinsic paramagnetic properties of Cu^{2+}.[45] When in situ generated PTNPy−Cu^{2+} complexes encountered Hcy, free PTNPy was released because of the stronger coordination interaction between Hcy and Cu^{2+},[38] resulting in that the fluorescence of PTNPy was restored. Based on the strategy, PTNPy can sequentially detect Cu^{2+} and Hcy with high selectivity. Further, PTNPy exhibited excellent biocompatibility and lysosome-targeting ability and was applied as an optical sensor for sequential imaging of Cu^{2+} and Hcy in HeLa cells.

2. RESULTS AND DISCUSSION

The synthetic route of PTNPy is shown in Scheme 1a. PTNPy was conveniently prepared by oxidative polymerization of *M*1 with *M*2 (the molar ratio of *M*1 to *M*2 is 1:1 in feed) in the presence of $FeCl_3$. The ^{1}H NMR spectrum of PTNPy (Figure S1) revealed clear peaks in the range of 8.41−7.16 ppm, corresponding to the characteristic aromatic hydrogen on pyridine rings in DPA-functionalized thiophene segments, and at ∼2.0 ppm, corresponding to the specific alkyl hydrogen (*a*, *a*′, *b*, and *b*′). An integral ratio ($I_{8.41-7.16}/I_{2.0}$) of 1.07 was consistent with the theoretical value (m:$n \approx 1$:2), indicative of the successful preparation of the target PTNPy. The polymer PTNPy can readily dissolve in deionized water, exhibiting strong yellow fluorescence with a fluorescence quantum efficiency (Φ) of 0.158 using rhodamine B as the reference (Φ = 0.73). The excellent water solubility of PTNPy, which meets the requirements of physiological applications, is related to the flexible substituent groups, especially quaternary ammonium salts on the side chains of polythiophenes.

The luminescence properties of PTNPy (100 μM) in the absence and presence of 15 different cations including Cu^{2+}, K^+, Na^+, Ag^+, Cd^{2+}, Fe^{2+}, Fe^{3+}, Al^{3+}, Hg^{2+}, Ca^{2+}, Co^{2+}, Mg^{2+}, Ni^{2+}, Pb^{2+}, and Zn^{2+} with the concentration of 100 μM in Tris−HCl buffer (2 mM, pH 7.4) was first studied. Among all tested ions, only Cu^{2+} can cause a remarkable fluorescence quenching of PTNPy (Figure 1a), suggesting the highly selective recognition ability of PTNPy toward Cu^{2+} ions. It was noted that just only Cu^{2+} can induce a slight red shift of the absorption spectra of PTNPy by around 19 nm along with a clear change of solution color from yellow to orange compared with the other tested metal ions (Figure S2), indicating a possible conformational transition of polymer backbone from random coil to planar conformation and even the formation of aggregates.[46] Therefore, the remarkable decrease in the fluorescence intensity of PTNPy in the presence of Cu^{2+} should be associated with two synergetic factors, that is, polymer aggregation and the paramagnetic properties of Cu^{2+}.

As can be seen from Figure 1b, as the Cu^{2+} concentrations increase, the fluorescence intensity of PTNPy in the Tris−HCl buffer solution gradually decreased with a significant blue shift (∼36 nm) of the emission peak. When 0.2 equiv of Cu^{2+} was added, a plateau was arrived, indicating that the saturation

https://doi.org/10.1021/acsomega.2c03691
ACS Omega 2022, 7, 34249−34257

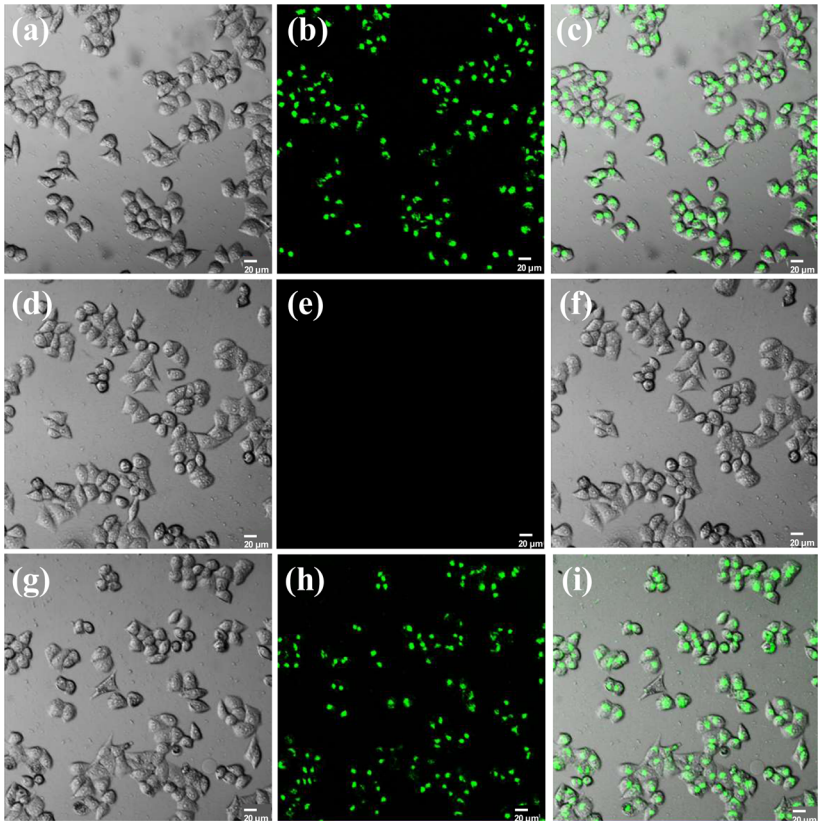

Figure 5. Fluorescence images of HeLa cells after incubating with PTNPy (a−c), PTNPy + Cu^{2+} (d−f), and PTNPy + Cu^{2+} + Hcy (g−i). (a,d,g) show bright-field images. (b) HeLa cells were cultured with PTNPy (20 μM) at 37 °C for 30 min. (e) PTNPy-loaded HeLa cells were treated with 4 μM Cu^{2+} ion at 37 °C for 10 min. (h) PTNPy and Cu^{2+}-loaded HeLa cells were cultured with Hcy (100 μM) at 37 °C for another 10 min. (c,f,i) show the merged images of HeLa cells. λ_{ex} = 405 nm and λ_{em} = 505−605 nm. Scale bars: 20 μm.

concentration of Cu^{2+} was 20 μM. The F_i/F_0 ratios of the fluorescence intensity of PTNPy at 550 nm were linearly proportional to [Cu^{2+}] in the range of 0−3 μM (inset in Figure 1c). The calibration curves were thus obtained to determine the limit of detection (LOD) of PTNPy toward Cu^{2+} to be 6.79 nM according to the standard $3\sigma/S$ method.[47] Clearly, PTNPy is a highly sensitive sensor for copper ion in an aqueous medium, showing one of lowest LOD values reported among fluorescence sensors for the detection of Cu^{2+} (Table S1). Further, Job's plot exhibited a 4:1 stoichiometry for the PTNPy−Cu^{2+} complex (Figure 1d) and that corresponding to the binding ratio of DPA groups to copper ions is about 5:2. Additionally, the binding constant of PTNPy with Cu^{2+} was estimated to be 1.42 × 10^5 M^{-1} based on the Benesi−Hildebrand equation (Figure S3), indicating strong affinity of PTNPy to Cu^{2+}.

Since other thiol-containing amino acids and peptides besides Hcy can coordinate well with Cu^{2+} ions through the affinity between copper and sulfur atoms,[48−50] we further checked the spectral response of PTNPy−Cu^{2+} complexes to various amino acids and peptides, including Ala, Ser, Thr, Cys, Pro, Phe, Trp, Glu, His, Val, Leu, Cys−Cys, Met, Lys, Arg, and GSH. The photoluminescence spectra of PTNPy−Cu^{2+} complexes were separately recorded in the presence of different analytes (Figure 2a). As displayed in Figure 2a, only slight spectral changes were observed in the case of the addition of 4 equiv of other amino acids and GSH. In sharp contrast, the addition of Hcy to PTNPy−Cu^{2+} complexes caused a remarkable spectral changes and a significant increase of fluorescence intensity at 550 nm by about 38 times (Figure 2b). The fluorescence spectra of PTNPy−Cu^{2+} complexes in the presence of 4 equiv of Hcy seem to be identical with that of free PTNPy (Figure S4), indicating that the fluorescence recovery is related to the complete release of PTNPy from PTNPy−Cu^{2+} complexes due to the strong chelation of Hcy with Cu^{2+}. Thus, PTNPy−Cu^{2+} complexes can selectively recognize Hcy over other sulfur-containing species such as Met and GSH in a perfect aqueous solution through the quick displacement mechanism.

Figure 2c shows the fluorescence titration spectra of PTNPy−Cu^{2+} complexes (100 μM) in Tris−HCl buffer (2 mM, pH 7.4) in the presence of various Hcy contents from 0 to 320 μM at a λ_{ex} of 400 nm. The quenched fluorescence of PTNPy−Cu^{2+} complexes was gradually restored with the increase of Hcy concentrations along with an obvious red shift of emission peaks by 40 nm. When the concentration of Hcy reached 3.2 equiv of PTNPy−Cu^{2+} complexes, the changes in fluorescence intensity became negligible, indicating the analyte−receptor saturation. Very importantly, the ratio of fluorescence intensity [$(F_i - F_0)/F_0$] depends linearly on the concentration of Hcy in the range of 0−300 μM with a correlation coefficient of 0.9990, where F_0 is the emission intensity of free PTNPy−Cu^{2+} complexes and F_i is the recorded emission intensities of PTNPy−Cu^{2+} complexes in the presence of Hcy with different concentrations (Figure 2d). Based on the result of fluorescence titration, the LOD for Hcy can be determined to be 9.64 × 10^{-8} M according to the standard $3\sigma/S$ method.[47] Therefore, PTNPy−Cu^{2+} complexes

https://doi.org/10.1021/acsomega.2c03691
ACS Omega 2022, 7, 34249−34257

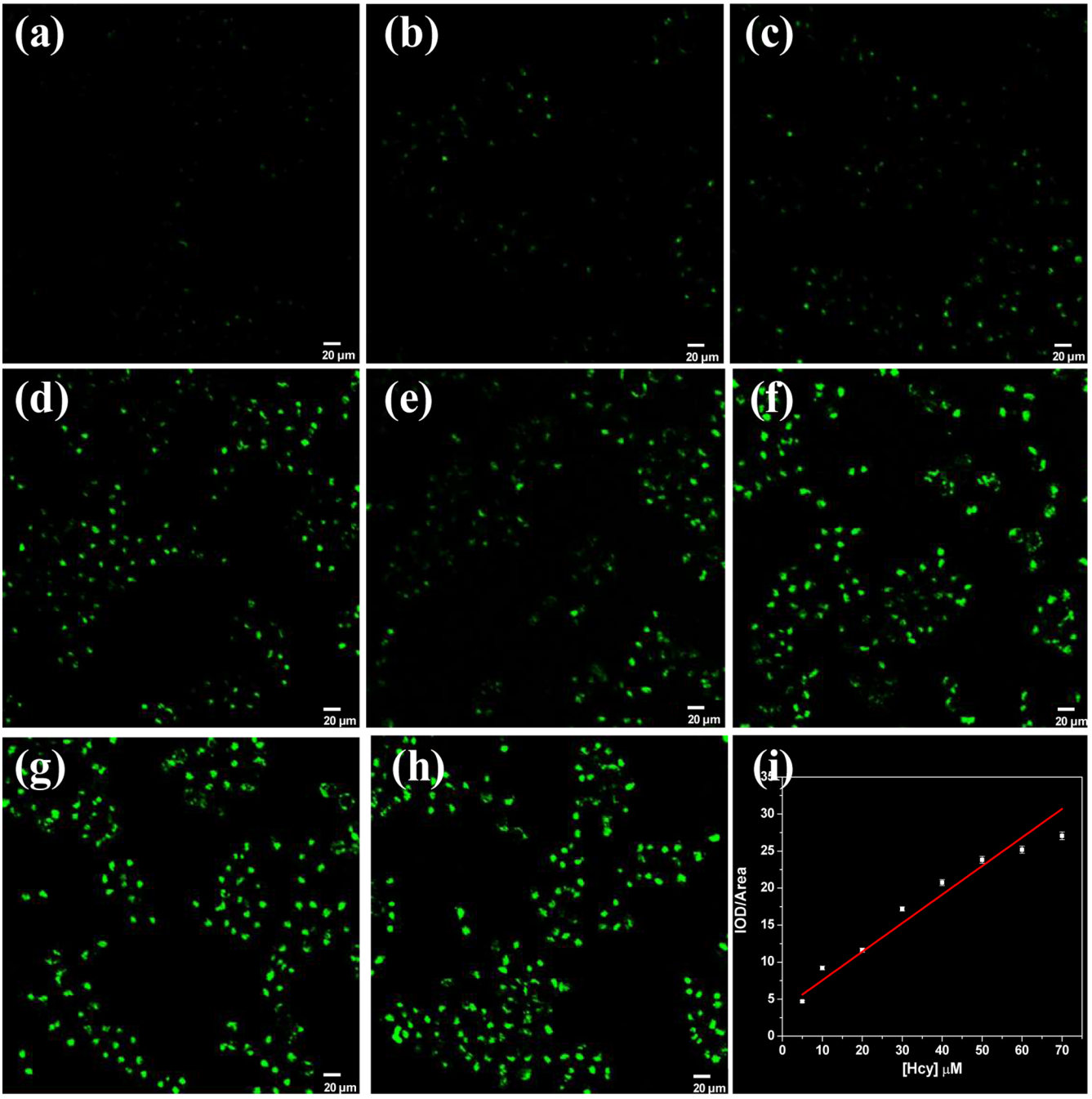

Figure 6. Confocal laser scanning microscopy (CLSM) images of PTNPy−Cu^{2+}-loaded HeLa cells incubated with different concentrations of Hcy. The concentrations of Hcy from (a−h) are 5, 10, 20, 30, 40, 50, 60, and 70 μM, respectively. (i) Plot of the fluorescence intensity density vs the concentration of Hcy. λ_{ex} = 405 nm and λ_{em} = 505−605 nm. Error bars represent the standard deviations of three independent experiments. Scale bars: 20 μm.

have huge potential for the quantitative determination of Hcy under physiological pH conditions.

As we know the cellular environment is very complex and there are various anions and cations such as K^+, Na^+, Ca^{2+}, Cl^-, CO_3^{2-}, SO_4^{2-}, and so on, the interference experiments were thus performed to evaluate the practical applicability of PTNPy sensor for the sequential detection of Cu^{2+} and Hcy in living cells. In this study, the Tris−HCl buffer (2 mM, pH 7.4) of PTNPy (100 μM) was treated with 1 equiv of the tested ions. Cu^{2+} (20 μM) was then added into the above solution, which was subsequently subjected to 4 equiv of Hcy. The fluorescence intensity at 550 nm at each case was separately recorded. As shown in Figure 3, in the presence of 1 equiv of other various substrates, the fluorescence of PTNPy can still be effectively quenched by 0.2 equiv of Cu^{2+} and almost completely recovered by Hcy subsequently. These results demonstrated that PTNPy is an excellent ON−OFF type optical sensor for Cu^{2+} with high selectivity over other competing ions, and the fluorescence of PTNPy−Cu^{2+} complexes can selectively response to Hcy even in a complex environment containing various ions as tested in this work.

The biocompatibility of PTNPy against HeLa cells was examined by a standard MTT assay (Figure S5). After 24 h of incubation, more than 94% of cells were viable at

https://doi.org/10.1021/acsomega.2c03691
ACS Omega 2022, 7, 34249−34257

concentration ranging from 0 to 100 μM PTNPy, indicating its slight toxicity. Colocalization experiments were carried out to assess the organelle-targeting ability of the sensor. HeLa cells were co-stained with PTNPy and a lysosome-targeting dye, that is, LysoTracker Red (Figure 4). PTNPy and LysoTracker Red showed a green and red fluorescence within lysosome, respectively (Figure 4a,b). The signal from PTNPy was well overlapped with that from LysoTracker Red with an overlap coefficient of 0.903 (Figure 4f). Therefore, PTNPy has good cell membrane permeability and can target the lysosome specifically. As a vital organelle, lysosome has the acidic physiological environment with pH 4.0−5.0. Thus, we further evaluated the effect of pH on the spectral characteristics of PTNPy and PTNPy−Cu^{2+} complexes. As shown in Figure S6, no significant changes in the fluorescence intensity of both were observed in the range of pH 4.0−8.0. These results indicated that PTNPy holds tremendous potential as a sensor to track Cu^{2+} and Hcy in the lysosome of living cells.

To verify the successive sensing capacity of the sensor PTNPy toward Cu^{2+} and Hcy in living cells, we explored their imaging applications in HeLa cells. After incubation with PTNPy (20 μM) for 30 min, HeLa cells showed bright green fluorescence (Figure 5a−c). The fluorescence of PTNPy was completed quenched after incubation with Cu^{2+} (4 μM) for 10 min (Figure 5d−f), demonstrating the formation of PTNPy−Cu^{2+} complexes within living cells. Subsequently, in situ generated PTNPy−Cu^{2+} complex-stained cells were treated by 100 μM Hcy, and bright green fluorescence was re-observed (Figure 5g−i). These results indicated that PTNPy can be effectively released from PTNPy−Cu^{2+} complexes when they encountered Hcy in the living cells.

Further, HeLa cells loaded by PTNPy and Cu^{2+} were cultured with Hcy at various concentrations such as 5, 10, 20, 30, 40, 50, 60, and 70 μM. After 30 min of incubation, the fluorescence images of cells were recorded (Figure 6). The restored fluorescence in HeLa cells with Hcy (70 μM) showed slight changes with prolonged irradiation time (0−100 s), demonstrating the good photostability of the sensor in living cells (Figure S7). More importantly, it was noted that the restored fluorescence intensity (the average fluorescence intensity density of 20 cells) was positively proportional to the Hcy concentration within the scope of 5−70 μM (Figure 6i). The calibration curves with R^2 = 0.957 can thus be obtained for possible quantitative determination of Hcy fluctuation in living cells.

3. CONCLUSIONS

In summary, we reported the design and synthesis of a new conjugated polymer-based fluorescence sensor (PTNPy) for the sequential detection of Cu^{2+} and Hcy in a 100% aqueous medium. PTNPy exhibits highly selective recognition ability toward Cu^{2+} ions over other metal ions by a fluorescence ON−OFF response with a low LOD of 6.79 nM for Cu^{2+}. The in situ generated PTNPy−Cu^{2+} complexes can be applied as a fluorescence sensor for quantitative detection and bio-imaging of Hcy in living cells. Benefiting from excellent biocompatibility and easy structural modification of polythiophenes, this work will pave a way for the future development of multifunctional optical sensors for the simultaneous detection of different target analytes through rational molecular design.

4. EXPERIMENTAL SECTION

4.1. Reagents and Materials. Hcy, L-Cys, reduced GSH, and other tested amino acids were provided by Tianjin Heowns Biochemical Technology Co., Ltd. (Tianjin, China). Copper(II) chloride dehydrate was obtained from Beijing Chemical Works (Beijing, China). 3-(3-Bromo-propoxy)-4-methyl-thiophene and *N*,*N*,*N*-trimethyl-3-((4-methylthiophen-3-yl)oxy)propan-1-aminium bromide were synthesized according to the procedure reported in our previous work.[46] 3-(4,5-Dimethylthiazol-2-yl)-2,5-diphenyl-tetrazolium bromide (MTT) was bought from Sigma-Aldrich (St. Louis, USA). Ultrapure water (18.6 M cm at 25 °C) was freshly prepared using a Millipore filtration system. The polymer concentration was calculated according to the repeat units (RUs).

4.2. Equipment and Methods. ^{1}H NMR spectra were recorded on a Bruker AV400 using residual solvent peak as a reference. Fluorescence analysis was carried out utilizing an F-4600 fluorescence spectrophotometer (Hitachi, Japan) equipped with a 1 cm quartz cell. UV analysis was recorded on a UV-3600 UV−vis spectrophotometer (Shimadzu, Japan). The pH values were determined using a Mettler Toledo Delta 320 pH meter. Cells were viewed with laser scanning confocal microscopy (Olympus FV1000-IX81). All images were digitized and analyzed with an Olympus FV1000-ASW.

4.3. CLSM Experiments. HeLa cells were grown in RPMI 1640 medium containing 10% FBS (fetal bovine serum) under a 5% CO_2 atmosphere at 37 °C. The cells were then planted on six-well plates and incubated overnight under the same conditions. After removing the medium, the cells were incubated with a solution of PTNPy in the medium (20 μM, 2 mL) for 30 min at 37 °C. The cells were rinsed with PBS three times and incubated with a solution of Cu^{2+} in culture media (4 μM, 2 mL) for 10 min at 37 °C. After washing with PBS three times, the medium was replaced by the medium (2 mL) with different concentrations of Hcy for 10 min at 37 °C. The cells were viewed using CLSM.

■ ASSOCIATED CONTENT

Supporting Information

The Supporting Information is available free of charge at https://pubs.acs.org/doi/10.1021/acsomega.2c03691.

Synthesis of monomer M1 and polymer PTNPy; spectral experiments; MTT assay; comparison of performance for the probes discussed in this work; and other spectral data (PDF)

■ AUTHOR INFORMATION

Corresponding Author

Yan Lu − *School of Materials Science & Engineering, Tianjin Key Laboratory for Photoelectric Materials and Devices, Key Laboratory of Display Materials & Photoelectric Devices, Ministry of Education, Tianjin University of Technology, Tianjin 300384, P. R. China;* orcid.org/0000-0003-1014-7842; Email: luyan@tjut.edu.cn

Authors

Lihua Liu − *School of Materials Science & Engineering, Tianjin Key Laboratory for Photoelectric Materials and Devices, Key Laboratory of Display Materials & Photoelectric Devices, Ministry of Education, Tianjin University of Technology, Tianjin 300384, P. R. China*

https://doi.org/10.1021/acsomega.2c03691
ACS Omega 2022, 7, 34249−34257

Hongfei Duan − *School of Materials Science & Engineering, Tianjin Key Laboratory for Photoelectric Materials and Devices, Key Laboratory of Display Materials & Photoelectric Devices, Ministry of Education, Tianjin University of Technology, Tianjin 300384, P. R. China*
Haohui Wang − *College of Chemistry, Nankai University, Tianjin 300071, P. R. China*
Jieru Miao − *School of Materials Science & Engineering, Tianjin Key Laboratory for Photoelectric Materials and Devices, Key Laboratory of Display Materials & Photoelectric Devices, Ministry of Education, Tianjin University of Technology, Tianjin 300384, P. R. China*
Zhihui Wu − *School of Materials Science & Engineering, Tianjin Key Laboratory for Photoelectric Materials and Devices, Key Laboratory of Display Materials & Photoelectric Devices, Ministry of Education, Tianjin University of Technology, Tianjin 300384, P. R. China*
Chenxi Li − *College of Chemistry, Nankai University, Tianjin 300071, P. R. China*

Complete contact information is available at: https://pubs.acs.org/10.1021/acsomega.2c03691

Notes

The authors declare no competing financial interest.

■ ACKNOWLEDGMENTS

This work was financially supported by the Natural Science Foundation of China (no. 52173010) and the Natural Science Foundation of Tianjin (no. 18JCZDJC34600).

■ REFERENCES

(1) Chen, X.; Zhou, Y.; Peng, X.; Yoon, J. Fluorescent and Colorimetric Probes for Detection of Thiols. *Chem. Soc. Rev.* **2010**, *39*, 2120−2135.
(2) Chen, H.; Tang, Y.; Lin, W. Recent Progress in the Fluorescent Probes for the Specific Imaging of Small Molecular Weight Thiols in Living Cells. *TrAC, Trends Anal. Chem.* **2016**, *76*, 166−181.
(3) Rihel, J. Copper on the Brain. *Nat. Chem. Biol.* **2018**, *14*, 638−639.
(4) Li, G.; Tao, F.; Liu, Q.; Wang, L.; Wei, Z.; Zhu, F.; Chen, W.; Sun, H.; Zhou, Y. Highly Selective and Reversible Water-Soluble Polymer Based-Colorimetric Chemosensor for Rapid Detection of Cu^{2+} in Pure Aqueous Solution. *New J. Chem.* **2016**, *40*, 4513−4518.
(5) Georgopoulos, P. G.; Roy, A.; Yonone-Lioy, M. J.; Opiekun, R. E.; Lioy, P. J. Environmental Copper: Its Dynamics and Human Exposure Issues. *J. Toxicol. Environ. Health, Part B* **2001**, *4*, 341−394.
(6) Dai, J.; Ma, C.; Zhang, P.; Fu, Y.; Shen, B. Recent Progress in the Development of Fluorescent Probes for Detection of Biothiols. *Dyes Pigm.* **2020**, *177*, 108321.
(7) Liu, W.; Chen, J.; Xu, Z. Fluorescent Probes for Biothiols Based on Metal Complex. *Coord. Chem. Rev.* **2021**, *429*, 213638.
(8) Khan, Z. G.; Patil, P. O. A Comprehensive Review on Carbon Dots and Graphene Quantum Dots Based Fluorescent Sensor for Biothiols. *Microchem. J.* **2020**, *157*, 105011.
(9) Zhang, J.; Wang, N.; Ji, X.; Tao, Y.; Wang, J.; Zhao, W. BODIPY-Based Fluorescent Probes for Biothiols. *Chem.—Eur. J.* **2020**, *26*, 4172−4192.
(10) Gaggelli, E.; Kozlowski, H.; Valensin, D.; Valensin, G. Copper Homeostasis and Neurodegenerative Disorders (Alzheimer's, Prion, and Parkinson's Diseases and Amyotrophic Lateral Sclerosis). *Chem. Rev.* **2006**, *106*, 1995−2044.
(11) Kaler, S. G. ATP7A-Related Copper Transport Diseases-Emerging Concepts and Future Trends. *Nat. Rev. Neurol.* **2011**, *7*, 15−29.
(12) Schalinske, K. L.; Smazal, A. L. Homocysteine Imbalance: a Pathological Metabolic Marker. *Adv. Nutr.* **2012**, *3*, 755−762.
(13) Narváez, J.; Maldonado, G.; Intriago, M.; Cárdenas, J.; Guerrero, R.; Neyro, J. L.; Ríos, C. Role of Homocysteine and Vitamin B in Bone Metabolism. *Rev. Colomb. Reumatol.* **2020**, *27*, 278−285.
(14) Gupta, M.; Meehan-Atrash, J.; Strongin, R. M. Identifying a Role for the Interaction of Homocysteine and Copper in Promoting Cardiovascular-Related Damage. *Amino Acids* **2021**, *53*, 739−744.
(15) Mansoor, M. A.; Bergmark, B.; Haswell, S. J.; Savage, I. F.; Evans, P. H.; Berge, R. K.; Svardal, A. M.; Kristensen, O. Correlation Between Plasma Total Homocysteine and Copper in Patients with Peripheral Vascular Disease. *Clin. Chem.* **2000**, *46*, 385−391.
(16) Dong, D.; Wang, B.; Yin, W.; Ding, X.; Yu, J.; Kang, Y. J. Disturbance of Copper Homeostasis is a Mechanism for Homocysteine-Induced Vascular Endothelial Cell Injury. *PLoS One* **2013**, *8*, 76209−76217.
(17) Borowczyk, K.; Suliburska, J.; Jakubowski, H. Demethylation of Methionine and Keratin Damage in Human Hair. *Amino Acids* **2018**, *50*, 537−546.
(18) Xia, Y.; Zhang, H.; Zhu, X.; Zhang, G.; Yang, X.; Li, F.; Zhang, X.; Fang, M.; Yu, J.; Zhou, H. A highly Selective Two-Photon Fluorescent Chemosensor for Tracking Homocysteine via Situ Reaction. *Dyes Pigm.* **2018**, *155*, 159−163.
(19) Zhang, X.; He, N.; Huang, Y.; Yu, F.; Li, B.; Lv, C.; Chen, L. Mitochondria-Targeting Near-Infrared Ratiometric Fluorescent Probe for Selective Imaging of Cysteine in Orthotopic Lung Cancer Mice. *Sens. Actuators, B* **2019**, *282*, 69−77.
(20) Gao, M.; Yu, F.; Lv, C.; Choo, J.; Chen, L. Fluorescent Chemical Probes for Accurate Tumor Diagnosis and Targeting Therapy. *Chem. Soc. Rev.* **2017**, *46*, 2237−2271.
(21) Peng, H.; Wang, K.; Dai, C.; Williamson, S.; Wang, B. Redox-Based Selective Fluorometric Detection of Homocysteine. *Chem. Commun.* **2014**, *50*, 13668−13671.
(22) Hakuna, L.; Escobedo, J. O.; Lowry, M.; Barve, A.; McCallum, N.; Strongin, R. M. A Photochemical Method for Determining Plasma Homocysteine with Limited Sample Processing. *Chem. Commun.* **2014**, *50*, 3071−3073.
(23) Escobedo, J. O.; Wang, W.; Strongin, R. M. Use of a Commercially Available Reagent for the Selective Detection of Homocysteine in Plasma. *Nat. Protoc.* **2006**, *1*, 2759−2762.
(24) Wu, Y.; Zhang, Y.; Wang, L.; Huyan, Y.; Li, H.; Pei, Z.; Tang, Y.; Sun, S.; Xu, Y. A Simple Ratiometric Fluorescent Sensor Selectively Compatible of Different Combinations of Characteristic Groups for Identification of Glutathione, Cysteine and Homocysteine. *Sens. Actuators, B* **2020**, *302*, 127181.
(25) Lee, H. Y.; Choi, Y. P.; Kim, S.; Yoon, T.; Guo, Z.; Lee, S.; Swamy, K. M. K.; Kim, G.; Lee, J. Y.; Shin, I.; Yoon, J. Selective Homocysteine Turn-On Fluorescent Probes and Their Bioimaging Applications. *Chem. Commun.* **2014**, *50*, 6967−6969.
(26) Qiu, X.; Jiao, X.; Liu, C.; Zheng, D.; Huang, K.; Wang, Q.; He, S.; Zhao, L.; Zeng, X. A Selective and Sensitive Fluorescent Probe for Homocysteine and Its Application in Living Cells. *Dyes Pigm.* **2017**, *140*, 212−221.
(27) Zhang, H.; Xu, L.; Chen, W.; Huang, J.; Huang, C.; Sheng, J.; Song, X. Simultaneous Discrimination of Cysteine, Homocysteine, Glutathione, and H_2S in Living Cells Through a Multisignal Combination Strategy. *Anal. Chem.* **2019**, *91*, 1904−1911.
(28) Shi, Y.; Yao, J.; Duan, Y.; Mi, Q.; Chen, J.; Xu, Q.; Gou, G.; Zhou, Y.; Zhang, J. 1,8-Naphthalimide-Cu(II) Ensemble Based Turn-On Fluorescent Probe for the Detection of Thiols in Organic Aqueous Media. *Bioorg. Med. Chem. Lett.* **2013**, *23*, 2538−2542.
(29) Okda, H. E.; El Sayed, S.; Otri, I.; Ferreira, R. C. M.; Costa, S. P. G.; Raposo, M. M. M.; Martínez-Máñez, R.; Sancenón, F. A Simple and Easy-to-Prepare Imidazole-Based Probe for the Selective Chromo-Fluorogenic Recognition of Biothiols and Cu(II) in Aqueous Environments. *Dyes Pigm.* **2019**, *162*, 303−308.
(30) Fu, Z.; Yan, L.; Zhang, X.; Zhu, F.; Han, X.; Fang, J.; Wang, Y.; Peng, Y. A Fluorescein-Based Chemosensor for Relay Fluorescence

Recognition of Cu(II) Ions and Biothiols in Water and Its Applications to a Molecular Logic Gate and Living Cell Imaging. *Org. Biomol. Chem.* **2017**, *15*, 4115−4121.
(31) Okda, H. E.; El Sayed, S.; Otri, I.; Ferreira, R. C. M.; Costa, S. P. G.; Raposo, M. M. M.; Martínez-Máñez, R.; Sancenón, F. 2,4,5-Triaryl imidazole Probes for the Selective Chromo-Fluorogenic Detection of Cu(II). Prospective Use of the Cu(II) Complexes for the Optical Recognition of Biothiols. *Polyhedron* **2019**, *170*, 388−394.
(32) Li, Q.; Guo, Y.; Shao, S. A BODIPY Based Fluorescent Chemosensor for Cu(II) Ions and Homocysteine/Cysteine. *Sens. Actuators, B* **2012**, *171-172*, 872−877.
(33) Li, Z.; Geng, Z.; Zhang, C.; Wang, X.; Wang, Z. BODIPY-Based Azamacrocyclic Ensemble for Selective Fluorescence Detection and Quantification of Homocysteine in Biological Applications. *Biosens. Bioelectron.* **2015**, *72*, 1−9.
(34) Jia, H.; Yang, M.; Meng, Q.; He, G.; Wang, Y.; Hu, Z.; Zhang, R.; Zhang, Z. Synthesis and Application of an Aldazine-Based Fluorescence Chemosensor for the Sequential Detection of Cu^{2+} and Biological Thiols in Aqueous Solution and Living Cells. *Sensors* **2016**, *16*, 79.
(35) Chao, D.; Zhang, Y. Aggregation Enhanced Luminescent Detection of Homocysteine in Water with Terpyridine-Based Cu^{2+} Complexes. *Sens. Actuators, B* **2017**, *245*, 146−155.
(36) Zhao, N.; Song, J.; Huang, Z.; Yang, X.; Wang, Y.; Zhao, L. Ratiometric Fluorescence Probe of Cu^{2+} and Biothiols by Using Carbon Dots and Copper Nanoclusters. *RSC Adv.* **2021**, *11*, 33662−33674.
(37) Guo, C.; Li, P.; Pei, M.; Zhang, G. A New Polythiophene Derivative-Based Fluorescent Sensor for Co^{2+}, Cu^{2+}, Cd^{2+}, and Its Complex with Cu^{2+} for Sensing Homocysteine and Glutathione. *Sens. Actuators, B* **2015**, *221*, 1223−1228.
(38) Zhang, W.; Zhang, H.; Wang, M.; Li, P.; Ding, C.; Zhang, W.; Wang, H.; Tang, B. Copolymer-Based Fluorescence Nanosensor for in situ Imaging of Homocysteine in the Liver and Kidney of Diabetic Mice. *Anal. Chem.* **2020**, *92*, 16221−16228.
(39) Zhu, C.; Liu, L.; Yang, Q.; Lv, F.; Wang, S. Water-Soluble Conjugated Polymers for Imaging, Diagnosis, and Therapy. *Chem. Rev.* **2012**, *112*, 4687−4735.
(40) Feng, X.; Liu, L.; Wang, S.; Zhu, D. Water-Soluble Fluorescent Conjugated Polymers and Their Interactions with Biomacromolecules for Sensitive Biosensors. *Chem. Soc. Rev.* **2010**, *39*, 2411−2419.
(41) Apostolova, M. D.; Bontchev, P. R.; Ivanova, B. B.; Russell, W. R.; Mehandjiev, D. R.; Beattie, J. H.; Nachev, C. K. Copper-Homocysteine Complexes and Potential Physiological Actions. *J. Inorg. Biochem.* **2003**, *95*, 321−333.
(42) Carrasco-Pozo, C.; Álvarez-Lueje, A.; Olea-Azar, C.; López-Alarcón, C.; Speisky, H. In Vitro Interaction Between Homocysteine and Copper Ions: Potential Redox Implications. *Exp. Biol. Med.* **2006**, *231*, 1569−1575.
(43) Linnebank, M.; Lutz, H.; Jarre, E.; Vielhaber, S.; Noelker, C.; Struys, E.; Jakobs, C.; Klockgether, T.; Evert, B. O.; Kunz, W. S.; Wüllner, U. Binding of Copper is a Mechanism of Homocysteine Toxicity Leading to COX Deficiency and Apoptosis in Primary Neurons, PC12 and SHSY-5Y Cells. *Neurobiol. Dis.* **2006**, *23*, 725−730.
(44) Emsley, A. M.; Jeremy, J. Y.; Gomes, G. N.; Angelini, G. D.; Plane, F. Investigation of the Inhibitory Effects of Homocysteine and Copper on Nitric Oxide-Mediated Relaxation of Rat Isolated Aorta. *Br. J. Pharmacol.* **1999**, *126*, 1034−1040.
(45) Liu, L.; Zhang, Q.; Wang, J.; Zhao, L.; Liu, L.; Lu, Y. A Specific Fluorescent Probe for Fast Detection and Cellular Imaging of Cysteine Based on a Water-Soluble Conjugated Polymer Combined with Copper(II). *Talanta* **2019**, *198*, 128−136.
(46) An, N.; Zhang, Q.; Wang, J.; Liu, C.; Shi, L.; Liu, L.; Deng, L.; Lu, Y. A New FERT-Based Ratiometric Probe for Fluorescent and Colorimetric Analyses of Adenosine 5′-triphosphate. *Polym. Chem.* **2017**, *8*, 1138−1145.
(47) Cheng, D.; Li, Y.; Wang, J.; Sun, Y.; Jin, L.; Li, C.; Lu, Y. Fluorescence and Colorimetric Detection of ATP Based on a Strategy of Self-Promoting Aggregation of a Water-Soluble Polythiophene Derivative. *Chem. Commun.* **2015**, *51*, 8544−8546.
(48) Zhang, L.; Cai, Q.; Li, J.; Ge, J.; Wang, J.; Dong, Z.; Li, Z. A Label-Free Method for Detecting Biothiols Based on Poly(Thymine)-Templated Copper Nanoparticles. *Biosens. Bioelectron.* **2015**, *69*, 77−82.
(49) Hao, W.; McBride, A.; McBride, S.; Gao, J. P.; Wang, Z. Y. Colorimetric and Near-Infrared Fluorescence Turn-On Molecular Probe for Direct and Highly Selective Detection of Cysteine in Human Plasma. *J. Mater. Chem.* **2011**, *21*, 1040−1048.
(50) Lee, S. A.; Lee, J. J.; Shin, J. W.; Min, K. S.; Kim, C. A Colorimetric Chemosensor for the Sequential Detection of Copper-(II) and Cysteine. *Dyes Pigm.* **2015**, *116*, 131−138.

https://doi.org/10.1021/acsomega.2c03691
ACS Omega 2022, 7, 34249−34257